

O  $\rightarrow$  S substitution on the potentials of Mo complexes containing otherwise identical ligands.<sup>22a,49b,56ac</sup> This effect, which renders O-ligated complexes poorer oxidants than their S-ligated analogues, is very large compared to, e.g., the 0.22 V difference between MoO<sub>2</sub>(tox)<sub>2</sub> and MoO<sub>2</sub>(ox)<sub>2</sub> in DMF.<sup>56ac</sup> Here the donor atom set also involves a 2S (tox = 8-mercaptoquinoline)  $\rightarrow$  2O (ox = 8-hydroxyquinoline) comparison. As will be seen,<sup>31</sup> the comparatively negative potential of MoO<sub>2</sub>(LNO<sub>2</sub>)(DMF) (which may also derive from structural differences) renders it inert to oxidation by Ph<sub>3</sub>P under conditions where MoO<sub>2</sub>(LNS<sub>2</sub>) stoichiometrically oxidizes this substrate. The oxo-transfer reactions of MoO<sub>2</sub>(LNS<sub>2</sub>) and MoO(LNS<sub>2</sub>)(DMF) are described in the following paper in this issue.<sup>31</sup>

**Acknowledgment.** This research was supported by NSF Grant CHE 81-06017. X-ray equipment used in this research was obtained by NSF Grant 80-00670.

**Registry No.** 1, 89959-09-1; 2, 89959-03-5; 3, 89959-04-6; 4, 89959-05-7; 5, 89975-14-4; 6, 89959-07-9; 7, 89959-08-0; 2,6-lutidine, 108-48-5; benzophenone, 119-61-9; diphenylmethanethiol, 831-91-4; 2,3-dihydropyran, 110-87-2; 2,6-bis(bromomethyl)pyridine, 7703-74-4.

**Supplementary Material Available:** Anisotropic temperature factors, calculated hydrogen atom coordinates, and calculated and observed structure factors for MoO<sub>2</sub>(LNO<sub>2</sub>)(Me<sub>2</sub>SO) and MoO<sub>2</sub>(LNS<sub>2</sub>) (33 pages). Ordering information is given on any current masthead page.

## A Model for the Active Sites of Oxo-Transfer Molybdoenzymes: Reactivity, Kinetics, and Catalysis

Jeremy M. Berg<sup>1</sup> and R. H. Holm\*

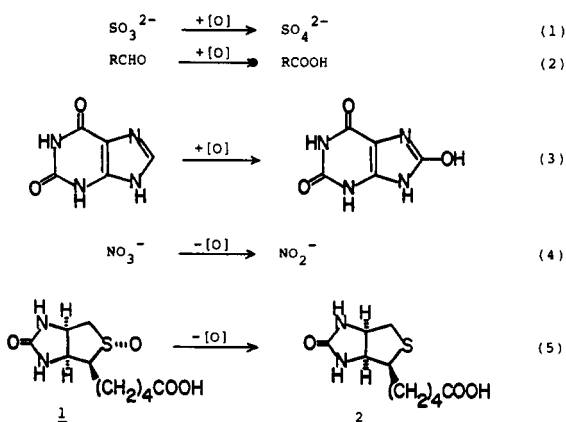
Contribution from the Department of Chemistry, Harvard University, Cambridge, Massachusetts 02138. Received August 10, 1984

**Abstract:** Oxidation-reduction reactions of substrates in systems containing the complexes Mo<sup>VI</sup>O<sub>2</sub>(LNS<sub>2</sub>) and Mo<sup>IV</sup>O(LNS<sub>2</sub>)(DMF) (LNS<sub>2</sub> = 2,6-bis(2,2-diphenyl-2-mercaptoethyl)pyridine) in DMF solutions at 23 °C have been investigated as models for the activities of certain oxo-transfer molybdoenzymes. The MoO<sub>1.2</sub>S<sub>2</sub>N coordination units are reasonable representations of this class of enzymes. MoO<sub>2</sub>(LNS<sub>2</sub>) reacts with Ph<sub>3</sub>P in a second-order process to yield MoO(LNS<sub>2</sub>)(DMF) and Ph<sub>3</sub>PO with the rate constant  $k_1 = 7 (1 \times 10^{-3} \text{ M}^{-1} \text{ s}^{-1})$ . MoO(LNS<sub>2</sub>)(DMF) reduces sulfoxides in a two-stage reaction involving equilibrium formation of the R<sub>2</sub>SO adduct ( $K = 4.2\text{--}16 \times 10^3$ ) followed by R<sub>2</sub>S formation ( $k_1 = 1.36\text{--}1.70 \times 10^{-3} \text{ s}^{-1}$ ). The small dependence of  $K$  and  $k_1$  on substrate structure suggests that the adduct is O-ligated to Mo(IV). These reactions exhibit the frequent enzymatic property of substrate saturation kinetics. One substrate is *d*-biotin *d*-(S-oxide), the natural substrate of the Mo-dependent enzyme biotin S-oxide reductase from *E. coli*, indicating the biological significance of the reactions. Evidence concerning this and other physiological sulfoxide reducing activities is summarized. Oxo transfers to and from substrate have been coupled to produce a catalytic system which turns over the reaction  $\text{Me}_2\text{SO} + \text{Ph}_3\text{P} \rightarrow \text{Me}_2\text{S} + \text{Ph}_3\text{PO}$ , in which Me<sub>2</sub>SO serves as a model substrate. No reaction is observed in the absence of the Mo catalyst. The initial catalytic rate is given by  $k[\text{MoO}_2(\text{LNS}_2)]$ , with  $k = 6 \times 10^{-3} \text{ M}^{-1} \text{ s}^{-1}$ . This rate is limited by the rate of reduction of MoO<sub>2</sub>(LNS<sub>2</sub>) by Ph<sub>3</sub>P. The sulfoxide reducing system developed here is characterized by substrate saturation kinetics, transformation of a biological substrate, and a well-defined catalytic cycle capable of turnover of hundreds of equivalents of a model substrate without intervention of a physiologically unrealistic  $\mu$ -oxo Mo(V) dimer. This system joins others recently devised in a broad development of reactivity models of metalloenzymes.

With the exception of nitrogenase,<sup>2</sup> the known molybdenum-containing enzymes catalyze reactions that, at least formally, are oxygen atom transfer processes. These oxo-transfer reactions are of two types: oxidation, involving the addition of an oxygen atom to substrate, and reduction, involving the removal of an oxygen atom from substrate. Examples are given as reactions 1-5, written without mechanistic implication. The properties and reactions

of oxo-transfer molybdoenzymes, including sulfite and aldehyde oxidases, xanthine oxidase/dehydrogenase, and nitrate reductase, have been reviewed.<sup>3-6</sup> *d*-Biotin *d*-(S-oxide) reductase, which catalyzes the reduction of the sulfoxide **1** to *d*-biotin (**2**) in reaction 5, is a more recently discovered Mo-dependent enzyme.<sup>7,8</sup> As will become evident, it is of particular relevance to the present research.

One approach to an understanding of the fundamental chemistry underlying enzymatic oxo-transfer reactions requires the development of well-characterized systems of synthetic Mo complexes capable of executing these or related reactions. In order for the information obtained from such systems to be most relevant to the enzyme problem, several additional criteria, previously enumerated,<sup>9-11</sup> must be met. First, the ligand environment should



(1) National Science Foundation Predoctoral Fellow, 1980-1983.

(2) Mortenson, L. E.; Thorneley, R. N. F. *Annu. Rev. Biochem.* **1979**, *48*, 387.

(3) Bray, R. C. In "The Enzymes"; Boyer, P. C., Ed.; Academic Press: New York, 1975; Vol. XII, Part B, Chapter 6.

(4) Bray, R. C. *Adv. Enzymol. Relat. Areas Mol. Biol.* **1980**, *51*, 107. (5) "Molybdenum and Molybdenum-Containing Enzymes"; Coughlan, M. P., Ed.; Pergamon Press: New York, 1980.

(6) "Molybdenum Chemistry of Biological Significance"; Newton, W. E., Otsuka, S., Eds.; Plenum Press: New York, 1980.

(7) del Campillo-Campbell, A.; Campbell, A. J. *Bacteriol.* **1982**, *149*, 469.

(8) del Campillo-Campbell, A.; Dykhuizen, D.; Cleary, P. P. *Methods Enzymol.* **1979**, *62*, 379.

(9) Berg, J. M.; Holm, R. H. *J. Am. Chem. Soc.* **1984**, *106*, 3035.

(10) Holm, R. H.; Berg, J. M. *Pure Appl. Chem.* **1984**, *56*, 1645.

(11) Berg, J. M.; Holm, R. H. *J. Am. Chem. Soc.*, preceding paper in this issue. This paper contains pertinent references to oxo-transfer molybdoenzymes and synthetic Mo complexes not cited here.

approximate those which have been implicated in enzyme sites from EXAFS<sup>12-14</sup> and EPR investigations.<sup>11</sup> Second, the complexes should be mononuclear and not form biologically irrelevant and potentially unreactive  $\mu$ -oxo Mo(V) dimers during the course of oxo-transfer reactions. Finally, the oxidized (Mo(VI)) and reduced (Mo(V,IV)) complexes should be interconvertible in both directions in order that catalytic cycles can be developed.

Limited progress has been made in the development of biologically relevant oxo-transfer systems based on synthetic Mo complexes. The complex  $\text{MoO}_2(o\text{-C}_6\text{H}_4(\text{S})\text{NHCH}_2)_2$  has been reported to oxidize  $\text{SO}_3^{2-}$ ,<sup>15</sup> but the nature of the oxidation product was not reported. The catalytic aerial oxidation of aldehydes to acids in the presence of  $\text{MoO}_2(\text{Cys-OEt})_2$  has been described,<sup>16</sup> but the role of the Mo complex is not well-defined. Other attempts to effect reaction 2 with dioxo Mo(VI) complexes have been unsuccessful.<sup>17-19</sup> No systems capable of the oxidation of xanthine (reaction 3) or other purines have been developed. Studies of the reduction of  $\text{NO}_3^-$  by monomeric Mo(V) species<sup>20-22</sup> reveal complicated reactions in which the initial product,  $\text{NO}_2$ , disproportionates to  $\text{NO}_2^-$  and  $\text{NO}_3^-$  in the presence of water. Several observations of the oxidations of monooxo Mo(IV,V) complexes with  $\text{NO}_3^-$  have been recorded.<sup>23,24</sup> This brief account, together with summaries of attempts to model enzymatic oxo-transfer reactions,<sup>24,25</sup> is sufficient to show that none of the reactions 1-4 has been even stoichiometrically reproduced with synthetic Mo complexes as reactants. That Mo-based oxo-transfer reaction which is the most general and thoroughly investigated is the oxidation of tertiary phosphines with dioxo Mo(VI) complexes.<sup>26,27</sup> This reaction is of much utility in the preparation of reduced Mo complexes and has been important in the development of our current understanding of the reactivity of oxo Mo species.<sup>26,28</sup>

Here we describe oxidative and reductive oxo-transfer systems which, in relation to enzymatic catalysis, have a number of desirable features. The monooxo Mo(IV) and dioxo Mo(VI) reactants possess  $\text{MoO}_2\text{S}_2\text{N}$  coordination units, which are reasonably consistent with Mo site structures from EXAFS.<sup>13,14</sup> Formation of a  $\mu$ -oxo dimer by these complexes is suppressed by ligand steric encumbrance. The Mo(IV) reactant is capable of reducing the biological substrate *d*-biotin *d*-(S-oxide) (1), as in reaction 5. A well-characterized catalytic oxo-transfer cycle has been developed. Finally, the reductive system mimics general enzymatic kinetic behavior, including the phenomenon of substrate saturation kinetics. This allows the independent examination of substrate binding and product formation and provides kinetics

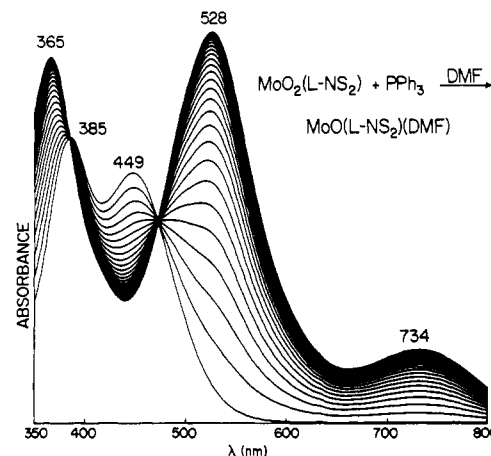


**Figure 1.** Spectral changes in the reaction of 2.5 mM  $\text{MoO}_2(\text{LNS}_2)$  and 2.5 equiv of  $\text{Ph}_3\text{P}$  in DMF solution at 23°C.

parameters that may be easily compared with enzymatic ones. Certain leading results of this investigation have been summarized.<sup>9,10</sup> The preceding paper in this issue<sup>11</sup> provides a full description of the synthesis of the Mo(IV, VI) compounds and several of their pertinent properties and the structure of the dioxo Mo(VI) complex.

## Experimental Section

**Preparation of Compounds.** [2,6-Bis(2,2-diphenyl-2-thioethyl)pyridinato]dioxomolybdenum(VI)<sup>11</sup> ( $\text{MoO}_2(\text{LNS}_2)$ ), [2,6-bis(2,2-diphenyl-2-thioethyl)pyridinato]([*N,N*-dimethylformamide)oxomolybdenum(IV)]<sup>11</sup> ( $\text{MoO}(\text{LNS}_2)(\text{DMF})$ ), [2,6-bis(2,2-diphenyl-2-oxoethyl)pyridinato](methanol)dioxomolybdenum(VI) ( $\text{MoO}_2(\text{LNO}_2)$ ), [2,6-bis(thiomethyl)pyridinato]dioxomolybdenum(VI),<sup>29</sup> and  $\text{MoO}_2(\text{S}_2\text{CNET}_2)_2$  were synthesized by published procedures. *d*-Biotin *d*-(S-oxide) (1) was prepared by the method of Melville<sup>31</sup> (mp 199–201 °C,  $[\alpha]_D^{25} +132^\circ$  (*c* 0.17, 0.1 N NaOH) [lit.<sup>31</sup> mp 200–203 °C,  $[\alpha]_D^{20} +130^\circ$ ). *d*-Biotin *l*-(S-oxide) was obtained by the procedure of Marti<sup>32</sup> (mp 240–241 °C,  $[\alpha]_D^{23} -39.8^\circ$  (*c* 0.28, 0.1 N NaOH) [lit. mp 239–240 °C,  $[\alpha]_D^{25} -39.5^\circ$ ]). The diastereomers of (*S*)-methionine *S*-oxide were prepared and separated by the method of Lavine<sup>33</sup> and were converted to their carbobenzyloxy derivatives according to Iselin.<sup>34</sup> Cbz-(*S*)-methionine *d*-(S-oxide), mp 111–113 °C,  $[\alpha]_D^{23} +47.5^\circ$  (*c* 0.41, ethanol) [lit.<sup>34</sup> mp 112–114 °C,  $[\alpha]_D^{27} +48.1^\circ$ ]; Cbz-(*S*)-methionine *l*-(S-oxide), mp 118–120 °C,  $[\alpha]_D^{23} -48.1^\circ$  (*c* 0.47, ethanol) [lit.<sup>34</sup> mp 115–117 °C,  $[\alpha]_D^{25} -47.7^\circ$ ]. Diphenyl sulfoxide (Aldrich) was recrystallized from benzene/hexanes. Dimethyl sulfoxide (Fisher) was distilled from  $\text{CaH}_2$  and stored under dinitrogen. Dimethyl sulfone (Crown Zellerbach) was recrystallized from ethyl acetate/hexanes. Samples of (*n*-Bu<sub>4</sub>N)(NO<sub>3</sub>) and (*n*-Bu<sub>4</sub>N)(NO<sub>2</sub>) (Fluka) were used as received.

**Measurements.** Optical rotations were determined with a Perkin-Elmer Model 241 polarimeter. All Mo-containing samples were prepared and measured under a pure dinitrogen atmosphere. UV-visible spectra were recorded on a Cary 219 spectrophotometer equipped with a thermostated cell compartment. <sup>31</sup>P NMR spectra were measured at 40.5 MHz with use of a Varian XL-100 spectrometer. Chemical shifts are reported relative to a 85%  $\text{H}_3\text{PO}_4$  external reference. Computations for data analysis were done with locally written programs.

## Results

The complexes  $\text{MoO}_2(\text{LNS}_2)$  (3) and  $\text{MoO}(\text{LNS}_2)(\text{DMF})$  (4) were synthesized<sup>11</sup> in order to examine oxo-transfer reactions to and from the substrate, respectively, by using molecules with biologically realistic coordination units and steric features designed to suppress  $\mu$ -oxo dimer formation.  $\text{MoO}_2(\text{LNS}_2)$  has a trigonal bipyramidal structure.<sup>11</sup> Crystals suitable for an X-ray structural determination of  $\text{MoO}(\text{LNS}_2)(\text{DMF})$  have not yet been obtained.

**Oxo Transfer from Mo(VI) to Substrate.** As shown in the preceding paper in this issue,<sup>11</sup>  $\text{MoO}(\text{LNS}_2)(\text{DMF})$  can be pre-

(12) Bordas, J.; Bray, R. C.; Garner, C. D.; Gutteridge, S.; Hasnain, S. S. *Biochem. J.* **1980**, *199*, 499.

(13) Cramer, S. P.; Wahl, R.; Rajagopalan, K. V. *J. Am. Chem. Soc.* **1981**, *103*, 7721.

(14) Cramer, S. P.; Solomonson, L. P.; Adams, M. W. W.; Mortenson, L. E. *J. Am. Chem. Soc.* **1984**, *106*, 1467.

(15) Spence, J. T.; Minelli, M.; Kroneck, P. *J. Am. Chem. Soc.* **1980**, *102*, 4538.

(16) Speier, G. *Inorg. Chim. Acta* **1979**, *33*, 139. (Cys-OEt = ethyl (S)-cysteinate)

(17) Miller, K. F.; Wentworth, R. A. D. *Inorg. Chem.* **1977**, *16*, 3385.

(18) Garner, C. D.; Durant, R.; Mabbs, F. E. *Inorg. Chim. Acta* **1977**, *24*, L29. A photochemical reaction to form benzoic acid from benzaldehyde and  $\text{MoO}_2(\text{S}_2\text{CNET}_2)_2$  is briefly described.

(19) Nakamura, A.; Nakayama, M.; Sugihashi, K.; Otsuka, S. *Inorg. Chem.* **1979**, *18*, 394.

(20) Garner, C. D.; Hyde, M. R.; Mabbs, F. E.; Routledge, V. I. *J. Chem. Soc., Dalton Trans.* **1975**, 1180.

(21) Taylor, R. D.; Todd, P. G.; Chasteen, N. D.; Spence, J. T. *Inorg. Chem.* **1979**, *18*, 44.

(22) Topich, J. *Inorg. Chem.* **1982**, *21*, 2079.

(23) Topich, J. *Inorg. Chim. Acta* **1980**, *46*, L97.

(24) Spence, J. T. In ref 5, Chapter 3. Spence, J. T.; Minelli, M.; Rice, C. A.; Chasteen, N. D.; Scullane, M. In ref 6, pp 263–278.

(25) Spence, J. T. *Coord. Chem. Rev.* **1983**, *48*, 59.

(26) Reynolds, M. S.; Berg, J. M.; Holm, R. H. *Inorg. Chem.* **1984**, *23*, 3057.

(27) (a) Topich, J.; Lyon, J. T., III. *Polyhedron* **1984**, *3*, 61; *Inorg. Chim. Acta* **1983**, *80*, L41. (b) Ueyama, N.; Yano, M.; Miyashita, H.; Nakamura, A.; Kamachi, M.; Nozakura, S. *J. Chem. Soc., Dalton Trans.* **1984**, 1447.

(28) Chen, G. J.-J.; McDonald, J. W.; Newton, W. E. *Inorg. Chem.* **1976**, *15*, 2612.

(29) Berg, J. M.; Holm, R. H. *Inorg. Chem.* **1983**, *22*, 1768.

(30) Moore, F. W.; Larson, M. L. *Inorg. Chem.* **1967**, *6*, 998.

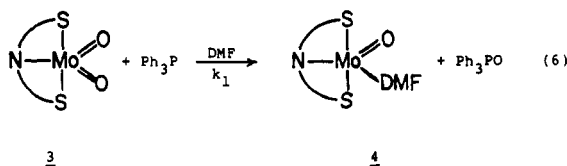
(31) Melville, D. B. *J. Biol. Chem.* **1954**, *203*, 495.

(32) Marti, F. B. Thesis, Eidgenössischen Technischen Hochschule, Zürich, 1983.

(33) Lavine, T. F. *J. Biol. Chem.* **1947**, *169*, 477.

(34) Iselin, B. *Helv. Chim. Acta* **1961**, *44*, 61.

pared by reaction 6. This reaction was monitored spectrophotometrically, as shown in Figure 1. Maxima at 385 and 449 nm



due to  $\text{MoO}_2(\text{LNS}_2)$  decrease, while the features of  $\text{MoO}(\text{LNS}_2)(\text{DMF})$  at 365, 528, and 734 nm increase, in intensity as the reaction proceeds. Clean isosbestic points are found at 386 and 473 nm. The final spectrum is identical with that of authentic  $\text{MoO}(\text{LNS}_2)(\text{DMF})$ .<sup>11</sup>

The kinetics of reaction 6 were investigated with  $\text{Ph}_3\text{P}:\text{MoO}_2(\text{LNS}_2)$  mole ratios of 2.2–3.0. At higher ratios a secondary reaction between the  $\text{Mo(IV)}$  complex and phosphine, leading to weakly colored solutions, becomes noticeable. Because of this limitation on the ratio of reactants, the kinetics data were treated in complete second-order form. The rate law 7 was integrated, yielding eq 8 where  $M$  and  $P$  are the initial concentrations of  $\text{MoO}_2(\text{LNS}_2)$  and  $\text{Ph}_3\text{P}$ , respectively. The concentration of the

$$\frac{d[\text{MoO}_2(\text{LNS}_2)]}{dt} = -k_1[\text{MoO}_2(\text{LNS}_2)][\text{Ph}_3\text{P}] \quad (7)$$

$$[\text{MoO}_2(\text{LNS}_2)](t) = \frac{(P - M)\text{Me}^{-k_1(P-M)t}}{P - \text{Me}^{-k_1(P-M)t}} \quad (8)$$

Mo(IV) product is given by eq 9. The value of rate constant  $k_1$  was determined by minimizing the function 10, where the absorbance values were taken at 530 ( $i = 1$ ) and 450 ( $i = 2$ ) nm.

$$[\text{MoO}(\text{LNS}_2)(\text{DMF})](t) = M - [\text{MoO}_2(\text{LNS}_2)] = \frac{MP(1 - e^{-k_1(P-M)t})}{P - Me^{-k_1(P-M)t}} \quad (9)$$

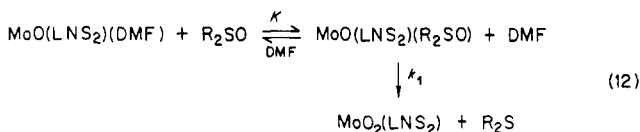
$$Q = \sum_{i=1}^2 \sum_j [A_{ij}^{\text{obsd}}(t_j) - A_{ij}^{\text{calcd}}(t_j)]^2 \quad (10)$$

The calculated absorbance at time  $t_j$ ,  $A^{\text{calcd}}(t_j)$ , is given by eq 11,

$$A_{ij}^{\text{calcd}}(t_j) = b(\epsilon_1^i)[\text{MoO}_2(\text{LNS}_2)] + \epsilon_2^i[\text{MoO}(\text{LNS}_2)(\text{DMF})] \quad (11)$$

in which  $b$  is the cell path length and the extinction coefficients<sup>11</sup> are  $\epsilon_1^1 = 600$ ,  $\epsilon_1^2 = 3900$ ,  $\epsilon_2^1 = 6280$ , and  $\epsilon_2^2 = 2170 \text{ M}^{-1} \text{ cm}^{-1}$ . For reaction 6,  $k = 7 (1) \times 10^{-3} \text{ M}^{-1} \text{ s}^{-1}$ .

**Oxo Transfer from Substrate to Mo(IV).** (a) **Sulfoxides.** MoO(LNS<sub>2</sub>)(DMF) has been found to react with Me<sub>2</sub>SO in DMF solution in the two-step reaction 12 to yield MoO<sub>2</sub>(LNS<sub>2</sub>) and Me<sub>2</sub>S. Spectrophotometric examination of the reaction revealed isosbestic points at 386 and 473 nm. The final spectrum is that



of authentic  $\text{MoO}_2(\text{LNS})_2$ .<sup>11</sup> The reaction is first order in the  $\text{Mo(IV)}$  complex, as shown by the linearity of plots of the absorbance function  $\ln(A_t - A_\infty)$  vs. time ( $t$ ) in experiments with  $>8$  equiv of  $\text{Me}_2\text{SO}$ . Reaction rates at various  $\text{Me}_2\text{SO}$  concentrations were determined from the slopes of these plots. The estimated standard deviation of rates obtained in this manner is  $4 \times 10^{-5} \text{ s}^{-1}$ . A plot of observed rates vs.  $[\text{Me}_2\text{SO}]$  is shown in Figure 2. At sufficiently high concentrations the rates become virtually independent of  $[\text{Me}_2\text{SO}]$ , i.e., substrate saturation kinetics obtain.

The foregoing observations are interpreted in terms of scheme 12. An equilibrium exists between the DMF- and sulfoxide-ligated Mo(IV) complexes. The sulfoxide complex undergoes an oxygen atom transfer reaction to generate MoO<sub>2</sub>(LNS<sub>2</sub>) and Me<sub>2</sub>S. Rate

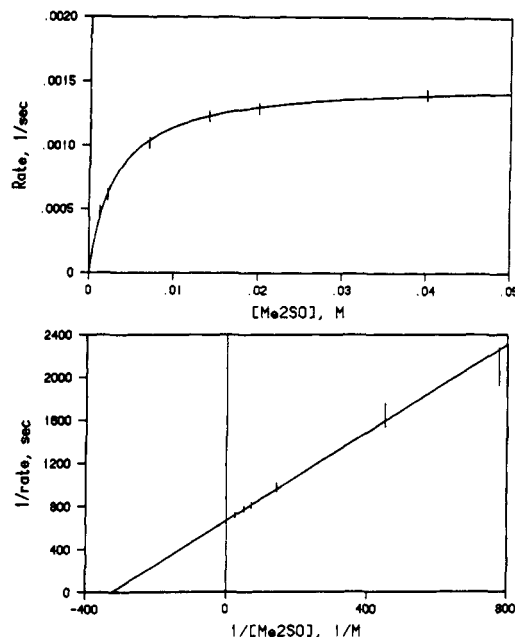


**Figure 2.** Upper: dependence of the rate of reaction of MoO(LNS)<sub>2</sub>-(DMF) and 8–250 equivalents of Me<sub>2</sub>SO in DMF solutions at 23 °C on [Me<sub>2</sub>SO]. Lower: plot of 1/rate vs. 1/[Me<sub>2</sub>SO] for the reaction in the upper figure.

law 13, in which ligand  $Y = \text{DMF} + \text{Me}_2\text{SO}$ , conforms to this scheme.

$$\frac{d[\text{MoO}(\text{LNS}_2)\text{Y}]}{dt} = -k_1[\text{MoO}(\text{LNS}_2)(\text{R}_2\text{SO})] = -k_1\left(\frac{K[\text{R}_2\text{SO}]}{K[\text{R}_2\text{SO}] + [\text{DMF}]}\right)[\text{MoO}(\text{LNS}_2)\text{Y}] \quad (13)$$

Thus,

$$[\text{MoO}(\text{LNS}_2)\text{Y}]t = [\text{Mo}]_0 e^{-Vt} \quad (14)$$

where

$$V = k_1 \left( \frac{K[R_2SO]}{K[R_2SO] + [DMF]} \right) \quad (15)$$

and  $[\text{Mo}]_0$  is the initial concentration of the Mo(IV) species. The values of  $K$  and  $k_i$  were determined by fitting eq 15 to the observed rate data. The function of eq 16 was minimized, where  $i$  is the index of different  $[\text{Me}_2\text{SO}]$  values and  $\sigma(V^{\text{obsd}})$  is the standard deviation in the value of  $V^{\text{obsd}}$ . The uncertainties in  $K$  and  $k_i$

$$\chi^2 = \sum_i \frac{1}{\sigma(V_i^{\text{obsd}})} (V_i^{\text{obsd}} - V_i^{\text{calcd}})^2 \quad (16)$$

were estimated by the changes in these parameters needed to increase the value of  $\chi^2$  by 1.<sup>35</sup> Values for Me<sub>2</sub>SO and other sulfoxide substrates are collected in Table I. The curve in Figure 2 (upper) is a plot of eq 15 with the derived values of  $K$  and  $k_1$ .

Alternatively, the rate data may be displayed in the form of a double-reciprocal plot, analogous to the Lineweaver-Burk plot often used in enzyme kinetics analysis. Inversion of eq 15 yields

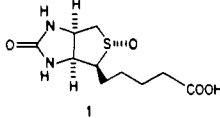
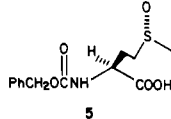
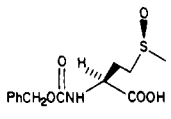
$$\frac{1}{V} = \frac{1}{k_1} + \frac{[\text{DMF}]}{k_1 K} \frac{1}{[\text{R}_2\text{SO}]} \quad (17)$$

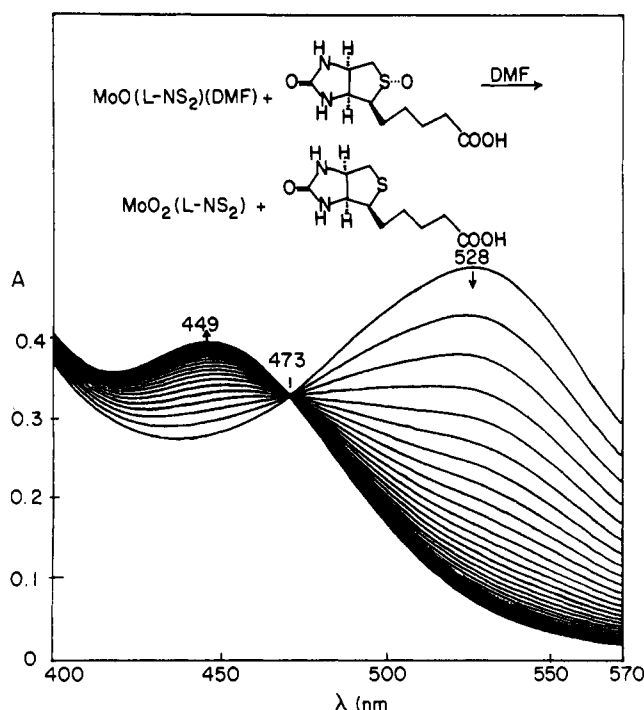
As seen in Figure 2, the  $\text{Me}_2\text{SO}$  reaction system displays the linear behavior required by eq 17.

MoO(LNS<sub>2</sub>)(DMF) reacts cleanly with a number of other sulfoxides (Table I). These reactions are also describable by scheme 12. Saturation kinetics are observed and were successfully

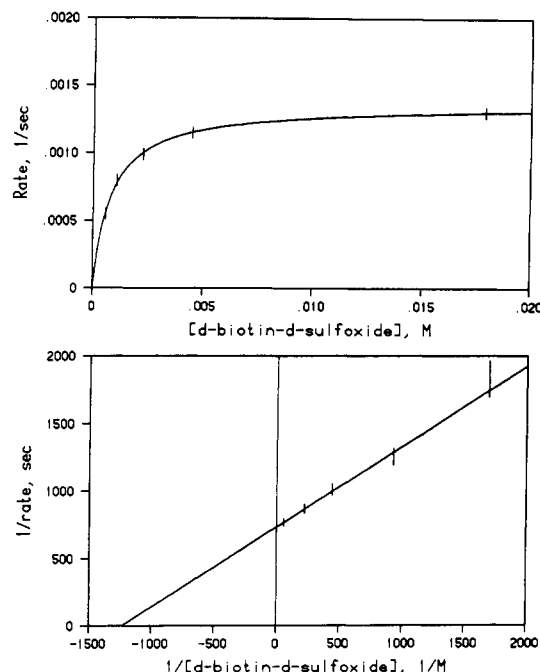
(35) Bevington, P. R. "Data Reduction and Error Analysis for the Physical Sciences;" McGraw-Hill: New York, 1969; pp 242-244.

Table I. Equilibrium Binding and Rate Constants for Reaction 12 at 23 °C

R <sub>2</sub> SO	K	k <sub>1</sub> , s <sup>-1</sup>
Me <sub>2</sub> SO	4.2 (3) × 10 <sup>3</sup>	1.50 (3) × 10 <sup>-3</sup>
Ph <sub>2</sub> SO	1.1 (1) × 10 <sup>4</sup>	1.43 (3) × 10 <sup>-3</sup>
 1	1.6 (1) × 10 <sup>4</sup>	1.36 (3) × 10 <sup>-3</sup>
 5	5.5 (4) × 10 <sup>3</sup>	1.63 (3) × 10 <sup>-3</sup>
 6	5.0 (4) × 10 <sup>3</sup>	1.70 (3) × 10 <sup>-3</sup>

Figure 3. Spectral changes in the reaction of 0.1 mM MoO(LNS<sub>2</sub>)(DMF) and 45 equiv of *d*-biotin *d*-(S-oxide) in DMF solution at 23 °C.

analyzed in terms of eq 13–17. The most significant observation is the reduction of *d*-biotin *d*-(S-oxide) (1), the natural substrate for the Mo-cofactor-dependent enzyme biotin S-oxide reductase.<sup>7,8</sup> As shown in Figure 3, the band at 528 nm due to the starting Mo(IV) complex decreases and the feature at 449 nm characteristic of MoO<sub>2</sub>(LNS<sub>2</sub>) increases in intensity as the reaction proceeds. A clean isosbestic point occurs at 473 nm. Kinetic plots in Figure 4 demonstrate saturation kinetics and the linear behavior of eq 17. *d*-Biotin was identified as the reaction product by thin-layer chromatography (*R<sub>f</sub>* = 0.25 vs. 0.11 for the starting sulfoxide, on silica plates eluted with dichloromethane). Our attention was drawn to (*S*)-methionine S-oxides ((*S*)-Met *S*-O) as possible substrates in view of the reports of their enzymatic reduction.<sup>36–39</sup> The sulfoxides<sup>33</sup> themselves were insufficiently

Figure 4. Upper: dependence of the rate of the reaction of MoO(LNS<sub>2</sub>)(DMF) and 6–180 equiv of *d*-biotin *d*-(S-oxide) in DMF solution at 23 °C on the sulfoxide concentration. Lower: plot of 1/rate vs. 1/[sulfoxide] for the reaction in the upper figure.

soluble to allow concentration variations adequate for detailed kinetics measurements. However, the carbobenzyloxy derivatives<sup>34</sup> Cbz-(*S*)-Met *l*-(S-O) (5) and Cbz-(*S*)-Met *d*-(S-O) (6, Table I) were sufficiently soluble for this purpose. The two diastereomers were cleanly reduced to Cbz-(*S*)-Met in reaction 12.

(b) **Other Substrates.** In a search for nitrate reductase activity, 0.3 mM MoO(LNS<sub>2</sub>)(DMF) was treated with 3–300 equiv of (*n*-Bu<sub>4</sub>N)(NO<sub>3</sub>) in DMF solution. Spectrophotometric examination of the reaction showed that MoO<sub>2</sub>(LNS<sub>2</sub>) was formed; perfect isosbestic points, as in Figures 1 and 3, did not develop. Plots of ln(*A<sub>t</sub>* - *A<sub>∞</sub>*) vs. *t* were essentially linear, indicating a reaction first order in the Mo(IV) complex. The reaction rate at 23 °C obtained from such plots is practically independent of [NO<sub>3</sub><sup>-</sup>] at 1–100 mM and has the value 1.3 × 10<sup>-3</sup> s<sup>-1</sup>. No nitrite could be detected<sup>40</sup> in the reaction products. Solutions of MoO(LNS<sub>2</sub>)(DMF) and (*n*-Bu<sub>4</sub>N)(NO<sub>2</sub>) in DMF were found to undergo a rapid, concentration-dependent reaction, leading initially to a pale yellow solution followed by complete decolorization. Addition of 2 equiv of (*n*-Bu<sub>4</sub>N)(NO<sub>2</sub>) to a solution of MoO<sub>2</sub>(LNS<sub>2</sub>) in DMF also caused rapid bleaching.

A solution of 0.2 mM MoO(LNS<sub>2</sub>)(DMF) and 50 equiv of Me<sub>2</sub>SO<sub>2</sub> showed a small decrease (<10%) in the intensity of the 528-nm absorption band over the first 10 min and no further change over an 8-h period. The slight spectral change at the outset may have been due to a Me<sub>2</sub>SO impurity in the sulfone. It is concluded that the Mo(IV) complex does not reduce or otherwise react with Me<sub>2</sub>SO<sub>2</sub>. MoO(LNS<sub>2</sub>)(DMF) does react with MoO<sub>2</sub>(S<sub>2</sub>CNEt<sub>2</sub>)<sub>2</sub>. At the initial concentrations [MoO(LNS<sub>2</sub>)(DMF)] = 0.1 mM and [MoO<sub>2</sub>(S<sub>2</sub>CNEt<sub>2</sub>)<sub>2</sub>] = 0.2 mM, the absorption spectrum after 20 min showed that MoO<sub>2</sub>(LNS<sub>2</sub>) was produced. The absorbance due to the other product, MoO(S<sub>2</sub>CNEt<sub>2</sub>)<sub>2</sub>,<sup>28,41</sup> is too small<sup>42</sup> to be clearly detectable at this concentration. However, at higher initial concentrations of MoO<sub>2</sub>(S<sub>2</sub>CNEt<sub>2</sub>)<sub>2</sub> (4.0 mM), substantial absorbance at 500–515 nm, characteristic of MoO<sub>3</sub>(S<sub>2</sub>CNEt<sub>2</sub>)<sub>4</sub><sup>42</sup> and not attributable to either complex of LNS<sub>2</sub>, was observed. These observations are

(36) Black, S.; Harte, E. M.; Hudson, B.; Wartofsky, L. *J. Biol. Chem.* **1960**, 235, 2910.

(37) (a) Ejiri, S.-I.; Weissbach, H.; Brot, N. *J. Bacteriol.* **1979**, 139, 161. (b) *Anal. Biochem.* **1980**, 102, 393.

(38) Brot, N.; Weissbach, L.; Werth, J.; Weissbach, H. *Proc. Natl. Acad. Sci. U.S.A.* **1981**, 78, 2155.

(39) Brot, N.; Weissbach, L. *Trends Biochem. Sci.* **1982**, 7, 137.

(40) Shinn, M. R. *Ind. Eng. Chem., Anal. Ed.* **1941**, 13, 33.

(41) Mitchell, P. C. H.; Scarle, R. D. *J. Chem. Soc., Dalton Trans.* **1975**, 2552.

(42) Newton, W. E.; Corbin, J. L.; Bravard, D. C.; Searles, J. E.; McDonald, J. W. *Inorg. Chem.* **1974**, 13, 1100.

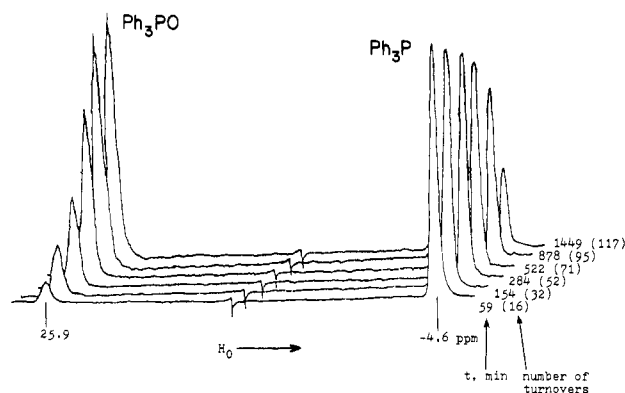
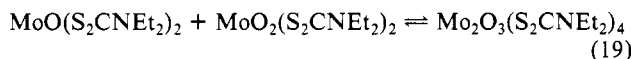
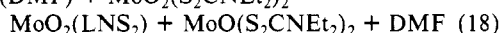


**Figure 5.**  $^{31}\text{P}$  NMR spectra showing the conversion of  $\text{Ph}_3\text{P}$  to  $\text{Ph}_3\text{PO}$  in a system containing initially 5.4 mM  $\text{MoO}_2(\text{LNS}_2)$ , 0.76 M  $\text{Ph}_3\text{P}$ , and 4.3 M  $\text{Me}_2\text{SO}$  in DMF. The elapsed time and number of turnovers prior to the recording of each spectrum are given.

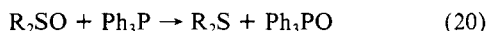
consistent with the sequential reactions 18 and 19. Reaction 19 has been independently demonstrated.<sup>42,43</sup>

**Catalysis of Oxo Transfer.** The occurrence of reactions 6 and 12 led to the possibility of their being coupled to produce a catalytic oxo-transfer cycle. When  $\text{MoO}_2(\text{LNS}_2)$  was placed in anaerobic  $\text{MoO}(\text{LNS}_2)(\text{DMF}) + \text{MoO}_2(\text{S}_2\text{CNEt}_2)_2 \rightarrow$



$\text{Me}_2\text{SO}$  or DMF/ $\text{Me}_2\text{SO}$  solutions containing up to 1500 equiv of  $\text{Ph}_3\text{P}$ , the solutions retained the characteristic orange color of the  $\text{Mo}(\text{VI})$  complex alone, and absorption spectra revealed no features unattributable to this species. Because  $\text{Me}_2\text{SO}$  was in excess over  $\text{Ph}_3\text{P}$ , this observation is that expected for coupled reactions under conditions where the concentration of the  $\text{Mo}(\text{VI})$  complex should be preserved. Substrate reaction products were identified as follows. In one experiment, 0.6 mM  $\text{MoO}_2(\text{LNS}_2)$  in  $\text{Me}_2\text{SO}$  solution was treated with 44 equiv of  $\text{Ph}_3\text{P}$ . During the reaction a stream of dinitrogen was passed through the reaction mixture and into an aqueous solution of  $\text{HgCl}_2$ , from which  $(\text{Me}_2\text{S})_2(\text{HgCl}_2)_3$ <sup>44</sup> precipitated. Quantitation of the washed and dried solid gave a 97% yield based on initial phosphine. The other reaction was readily identified and quantitated by  $^{31}\text{P}$  NMR spectroscopy. As shown in Figure 5, the signal at 25.9 ppm due to  $\text{Ph}_3\text{PO}$  increases and the  $\text{Ph}_3\text{P}$  signal decreases in intensity as the reaction proceeds.

These observations establish catalysis of reaction 20 ( $\text{R} = \text{Me}$ ). In the absence of any catalyst,  $\text{Me}_2\text{SO}$  and  $\text{Ph}_3\text{P}$  do not react for at least 1 h at 189 °C.<sup>44</sup> It was demonstrated by  $^{31}\text{P}$  NMR



spectroscopy that none of the sulfoxides in Table I underwent detectable reaction with excess  $\text{Ph}_3\text{P}$  in DMF solutions at room temperature. If phosphine oxidation is rate-limiting under these conditions, the consumption of  $\text{Ph}_3\text{P}$  should be first order in both phosphine and  $\text{MoO}_2(\text{LNS}_2)$ . Because the regeneration of this complex is relatively fast, its concentration should be essentially constant throughout the reaction. Thus, the disappearance of  $\text{Ph}_3\text{P}$  should follow rate eq 21, where the subscript denotes initial concentration. This relationship is also expressible as eq 22, plots of which are presented in Figure 6. The concentration term was

$$[\text{Ph}_3\text{P}] = [\text{Ph}_3\text{P}]_0 e^{-k[\text{MoO}_2(\text{LNS}_2)]t} \quad (21)$$

$$\ln \left( \frac{[\text{Ph}_3\text{P}] + [\text{Ph}_3\text{PO}]}{[\text{Ph}_3\text{P}]} \right) = k[\text{MoO}_2(\text{LNS}_2)]t \quad (22)$$

evaluated from integrated intensities of  $^{31}\text{P}$  resonances. Initial slopes are  $9.9 \times 10^{-6}$ ,  $1.7 \times 10^{-5}$ , and  $3.4 \times 10^{-5} \text{ s}^{-1}$  for  $[\text{MoO}_2(\text{LNS}_2)] = 1.7$ , 3.0, and 5.4 mM, respectively.

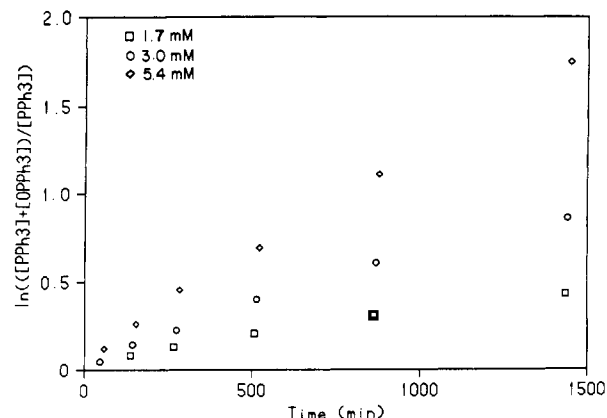


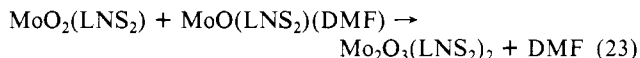
**Figure 6.** Plots of  $\ln ([\text{Ph}_3\text{P}] + [\text{Ph}_3\text{PO}]) / [\text{Ph}_3\text{P}]$  vs. time for systems containing initially 1.7, 3.0, and 5.4 mM  $\text{MoO}_2(\text{LNS}_2)$ , 0.76 M  $\text{Ph}_3\text{P}$ , and 4.3 M  $\text{Me}_2\text{SO}$  in DMF. The concentration variable was evaluated from integration of  $^{31}\text{P}$  signals such as those in Figure 5.

$\text{O}_2(\text{LNS}_2)] = 1.7$ , 3.0, and 5.4 mM, respectively. Slopes divided by the  $\text{Mo}(\text{VI})$  complex concentration are nearly constant and give  $k = 6 \times 10^{-3} \text{ M}^{-1} \text{ s}^{-1}$ .

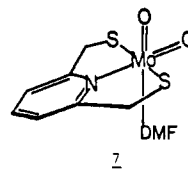
Catalytic systems do show signs of decreased activity at sufficiently long times. The plots in Figure 6 deviate from linearity. After 24 h, the slopes (preceding order) have decreased to  $3.4 \times 10^{-6}$ ,  $7.4 \times 10^{-6}$ , and  $1.9 \times 10^{-5} \text{ s}^{-1}$ . The lowered activity is paralleled by a decay of absorption intensity. For the system in Figure 6 with 1.0 mM  $\text{MoO}_2(\text{LNS}_2)$ , a 20% decrease in spectral intensity was observed after 6 h.

## Discussion

**Biological Relevance of  $\text{Mo}(\text{VI}, \text{IV})$  Complexes.**  $\text{MoO}_2(\text{LNS}_2)$  and  $\text{MoO}(\text{LNS}_2)(\text{DMF})$  were designed to contain biologically credible coordination units, steric properties sufficient to suppress  $\mu$ -oxo dimerization, and labile sites for possible substrate binding. On the basis of  $\text{Mo}$  EXAFS results,<sup>13,14</sup> the  $\text{MoO}_{1.2}\text{S}_2\text{N}$  units are credible approaches to those present in several oxo-transfer enzymes. The existence of sharp isosbestic points in the spectra of reactions 6 and 12 (Figures 1 and 3), together with a prior NMR proof<sup>9</sup> that the experimental reaction stoichiometry of the system  $\text{MoO}_2(\text{LNS}_2)/\text{Ph}_3\text{P}$  in DMF is consistent only with formation of  $\text{MoO}(\text{LNS}_2)(\text{DMF})$ , eliminates the  $\mu$ -oxo dimerization reaction 23 from further consideration. In contrast, reaction of the related



complex **7**<sup>29</sup> with  $\text{Ph}_3\text{P}$  in DMF gave a brown, sparingly soluble solid with  $\nu_{\text{MoO}} = 945 \text{ 790 cm}^{-1}$ . This compound was shown to



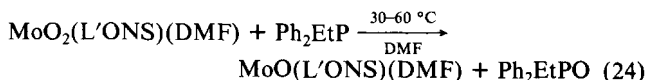
be the  $\mu$ -oxo dimer  $\text{Mo}_2\text{O}_3(\text{C}_5\text{H}_5\text{N}(\text{CH}_2\text{S})_2)_2$  by its identity with the reaction product of  $\text{Mo}_2\text{O}_3(\text{acac})_4$  and 2,6-bis(mercapto-methyl)pyridine. Evidently, the six-membered chelate rings and the *gem*-diphenyl groups, which protrude in the direction of the  $\text{Mo}=\text{O}$  bonds, provide a steric hindrance sufficient to suppress reaction 23.<sup>45</sup> The structure of  $\text{MoO}_2(\text{LNS}_2)$ , with emphasis on its steric features, is described elsewhere.<sup>11</sup> While this work was

(43) Matsuda, T.; Tanaka, K.; Tanaka, T. *Inorg. Chem.* **1979**, *18*, 454.

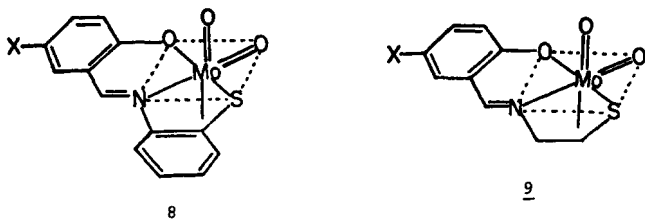
(44) Szmant, H. E.; Cox, O. J. *Org. Chem.* **1966**, *31*, 1595.

(45) We have not actually proven, by the synthesis of  $\text{Mo}(\text{VI}, \text{IV})$  complexes of (unknown) 2,6-bis(thioethyl)pyridine, that the steric bulk of the phenyl groups in  $\text{MoO}_2(\text{LNS}_2)$  and  $\text{MoO}(\text{LNS}_2)(\text{DMF})$  is responsible for the lack of occurrence of reaction 23. Steric inhibition of  $\mu$ -oxo dimerization is, however, supported by the X-ray structure of  $\text{MoO}_2(\text{LNS}_2)$ <sup>11</sup> and inspection of space-filling molecular models. We do not claim that a  $\mu$ -oxo  $\text{Mo}(\text{V})$  dimer containing the  $\text{LNS}_2$  ligand cannot exist—only that it does not form for kinetic or thermodynamic reasons under the conditions employed.

in progress Topich and Lyon<sup>27a</sup> reported that a series of solvated, tridentate salicylaldiminato dioxo Mo(VI) complexes **8** and **9**, containing one thiolate ligand, underwent reaction 24 with no evidence of  $\mu$ -oxo dimer formation. Inasmuch as these complexes



do not appear to be hindered, the reason for lack of dimerization is unclear. Very recently, Subramanian et al.<sup>46</sup> have prepared



a series of sterically hindered dioxo Mo(VI) and monooxo Mo(IV) complexes, mainly with O and N binding sites. The oxo-transfer reactivity properties of these species were not reported.

The absence of reaction 23 permits evaluation of rate constants for oxo transfer to and from the substrate without resorting to the more complicated kinetics analysis required when such a reaction (e.g., eq 19) is operative and reversible.<sup>26</sup> The value  $k_1 = 7(1) \times 10^{-3} \text{ M}^{-1} \text{ s}^{-1}$  for reaction 6 at 23 °C is an order of magnitude smaller than for  $\text{MoO}_2(\text{S}_2\text{CNET}_2)_2$  and  $\text{Ph}_3\text{P}$  in 1,2- $\text{C}_2\text{H}_4\text{Cl}_2$  at 25 °C ( $7.3(1) \times 10^{-2} \text{ M}^{-1} \text{ s}^{-1}$ ).<sup>26</sup> It is substantially larger than the values  $8.4\text{--}19.6 \times 10^{-4} \text{ M}^{-1} \text{ s}^{-1}$ <sup>27a</sup> for reaction 24 with **8** and the more reactive phosphine.  $\text{Ph}_3\text{P}$  was reported not to react at any reasonable rate under these conditions. A common feature of these complexes is the presence of sulfur ligands. To examine the effect of thiolato ligands on reactivity,  $\text{MoO}_2(\text{LNO}_2)(\text{DMF})$ <sup>11</sup> ( $E_{\text{pc}} = -1.8 \text{ V}$ ), the alkoxide analogue of  $\text{MoO}_2(\text{LNS}_2)$  ( $E_{\text{pc}} = -0.88 \text{ V}$  vs. SCE), was treated with  $\text{Ph}_3\text{P}$  in DMF solution at ambient temperature. Whereas reaction 6 proceeds readily, no reaction was observed with  $\text{MoO}_2(\text{LNO}_2)(\text{DMF})$ . The indicated peak potentials for irreversible one-electron reductions of the Mo(VI) complexes<sup>11</sup> differ by  $\sim 0.9 \text{ V}$ , with  $\text{MoO}_2(\text{LNO}_2)(\text{DMF})$  being the poorer oxidant. Similarly, the corresponding reductions of **8** and **9** occur at  $E_{\text{pc}}$  values 0.1–0.3 V less negative than those of their oxygen analogues.<sup>47</sup> While such reduction reactions are not likely to be of physiological significance, the potentials do raise the possibility that one function of thiolate ligands, two or three of which are present in the oxidized forms of oxo-transfer enzymes,<sup>13,14</sup> is to render dioxo Mo(VI) a physiologically competent oxidant. Topich and Lyon<sup>27a</sup> have shown that variation of group X in **8** gives a linear relationship between the rate constants of reaction 24 and  $E_{\text{pc}}$  values. At least by this measure, the stronger oxidants react faster.

**Sulfoxide Biochemistry.** The significance of reduction of sulfoxides by Mo complexes lies in the discovery that *d*-biotin *d*-(S-oxide) reductase of *E. coli* is a Mo cofactor-dependent enzyme.<sup>7</sup> The known genetic characteristics of the cofactor permit this conclusion even though the enzyme has yet to be substantially purified. In particular, mutations in three genes which caused diminished biotin S-oxide reductase activity in *E. coli* have been assigned to genes involved in the expression of nitrate reductase activity, apparently by participating in the synthesis or processing of the Mo cofactor. The conclusion is further substantiated by the finding that the presence of tungstate in the growth medium significantly decreases the amount of biotin S-oxide reductase activity present.<sup>7</sup> The function of this enzyme is apparently to recover the vitamin from its adventitiously oxidized form.

Two other classes of biological sulfoxide reducing activities have been investigated. First, several methionine sulfoxide reducing enzymes have been purified, one from yeast<sup>36</sup> and two from *E.*

*coli*,<sup>37b,38</sup> and others have been detected in different organisms.<sup>38,48,49</sup> These systems are of considerable interest because of the possible role of Met S-O residues in affecting the biological activity of peptides and proteins.<sup>39</sup> The three enzymes that have been at least partially purified show contrasting properties. The yeast enzyme is specific for one of the four Met S-O diastereomers, viz., (S)-Met *l*-(S-O).<sup>36</sup> One of the *E. coli* enzymes does not discriminate between (S)-Met *d*-(S-O) and (S)-Met *l*-(S-O).<sup>37a</sup> The other appears to act only on Met S-O residues bound in peptides.<sup>38</sup> It is not known if any of these enzymes is Mo-dependent.

Second, the reduction of  $\text{Me}_2\text{SO}$  to  $\text{Me}_2\text{S}$  by a number of different organisms has been reported.<sup>50</sup> Interest in this enzymatic reaction is generated by the possible environmental and medicinal roles of  $\text{Me}_2\text{SO}$ <sup>50</sup> and by the formation of  $\text{Me}_2\text{S}$ , a component of beer flavor, during fermentation.<sup>51,52</sup> In some cases it appears that the  $\text{Me}_2\text{SO}$  reducing activity is due to biotin<sup>50</sup> or Met S-O<sup>52</sup> reduction systems, but further work is required to elucidate any relationships between these processes. Interestingly, however, some of the mutants used in the identification of Mo-co dependence of *E. coli* biotin S-oxide reductase also show substantially reduced  $\text{Me}_2\text{SO}$  reduction activity vs. wild-type organisms.<sup>50</sup>

**Sulfoxide Reduction Systems.** The sulfoxide reduction reaction 12 occurs with the five substrate molecules in Table I and would doubtless occur with numerous other sulfoxides as well. That *d*-biotin *d*-(S-oxide) (**1**) is a substrate demonstrates that  $\text{MoO}(\text{LNS}_2)(\text{DMF})$  can execute biologically relevant oxo-transfer reactions. Given the reduction of the protected Met S-O derivatives **5** and **6**, this statement would be further strengthened if methionine S-oxide reductases are shown to be Mo-dependent enzymes.

The kinetics properties of the sulfoxide reducing system make it especially attractive as an enzyme model. Substrate saturation kinetics is a frequent aspect of enzymatic reactions. In such a case, substrate binding in an equilibrium process occurs prior to conversion of the substrate complex to products, as shown for the model system in reaction 12. The kinetics parameters in Table I reveal several important characteristics of this system. (i) Equilibrium constants reflect fairly tight binding of sulfoxide to Mo(IV) and correspond to a  $\sim 5 \text{ kcal/mol}$  higher binding energy for sulfoxides vs. DMF. Solvent and substrate binding to  $\text{MoO}(\text{LNS}_2)$  is promoted by the presence of only four nonlabile ligands, a design aspect of the molecule. (ii) Both the equilibrium constants and oxo-transfer rate constants have narrow ranges, viz.,  $(4.2\text{--}16) \times 10^3$  and  $(1.36\text{--}1.70) \times 10^{-3} \text{ s}^{-1}$ , respectively. Given the differences in local structure around the sulfur atom, this result implies that the substrate binds to Mo(IV) through the sulfoxide oxygen atom. (iii) While reaction rates are modest, they compare favorably with the turnover rate for *E. coli* methionine S-oxide reductase after purification to near-homogeneity. This enzyme has a highest reported specific activity of 4521 pmol of Met S-O reduced/mg of protein/10 min,<sup>37b</sup> which with  $M_r = 21\,000$  gives  $k_1 = 1.6 \times 10^{-4} \text{ s}^{-1}$ . (iv) The quantity  $k_1/K_m$ , where  $K_m = [\text{DMF}]/K$ , is effectively a second-order rate constant for sulfoxide reduction. For  $\text{Me}_2\text{SO}$ , this has the value  $0.5 \text{ M}^{-1} \text{ s}^{-1}$ , over 3 orders of magnitude greater than that observed with  $\text{MoO}(\text{S}_2\text{CNET}_2)_2$  ( $1.6 \times 10^{-4} \text{ M}^{-1} \text{ s}^{-1}$ ),<sup>26</sup> the only other oxo Mo(IV) complex which has been shown to reduce  $\text{Me}_2\text{SO}$ .

Several other observations are pertinent. With regard to (ii), *d*-biotin *l*-(S-oxide) is not an enzyme substrate in at least some organisms,<sup>53</sup> and, compared to its epimer **1**, it has been found to be more resistant to reduction by  $\text{Zn/HCl}$ .<sup>31</sup> These results are consistent with the structure of this isomer, as readily deduced

(46) Subramanian, P.; Spence, J. T.; Ortega, R.; Enemark, J. H. *Inorg. Chem.* **1984**, *23*, 2564.

(47) Topich, J.; Lyon, J. T., III. *Polyhedron* **1984**, *3*, 55.

(48) Doney, R. C.; Thompson, J. F. *Biochim. Biophys. Acta* **1966**, *124*, 39.

(49) Aymard, C.; Seyer, L.; Cheftel, J.-C. *Agric. Biol. Chem.* **1979**, *43*, 1869.

(50) Zinder, S. H.; Brock, T. D. *J. Gen. Microbiol.* **1978**, *105*, 335.

(51) Anness, B. J.; Bamforth, C. W.; Wainwright, T. J. *Inst. Brew.* **1979**, *85*, 346.

(52) Anness, B. J. *J. Inst. Brew.* **1980**, *86*, 134.

(53) Melville, D. B.; Genghof, D. S.; Lee, J. M. *J. Biol. Chem.* **1954**, *208*, 503.

from that of **1**.<sup>54</sup> Compared to the latter, approach to the sulfoxide oxygen atom is hindered by the *cis* position of the pentanoic acid side chain and by the conformation of the biotin framework. The low solubility of *d*-biotin *l*-(S-oxide) in DMF (<1 mg/mL, 23 °C) precluded a complete kinetics investigation. However, it was established that this isomer reacted with MoO(LNS<sub>2</sub>)(DMF) at a much slower rate than does **1** at similar concentrations. Concerning (iii), while it is not possible to calculate a precise turnover number for yeast Met S-O reductase from available data,<sup>36</sup> estimates indicate that this enzyme is several orders of magnitude faster than the *E. coli* enzyme.

**Reaction with Nitrate.** The Mo-containing product of the reaction of MoO(LNS<sub>2</sub>)(DMF) and NO<sub>3</sub><sup>-</sup> in DMF is largely MoO<sub>2</sub>(LNS<sub>2</sub>). The rate of appearance of this species is essentially independent of [NO<sub>3</sub><sup>-</sup>] over a wide range, suggesting that NO<sub>3</sub><sup>-</sup> coordination is required prior to reaction. However, no NO<sub>2</sub><sup>-</sup> was found in the final solutions, indicating that, if formed, it reacted quickly to give other products. It was found that NO<sub>2</sub><sup>-</sup> reacted rapidly with both MoO<sub>2</sub>(LNS<sub>2</sub>) and MoO(LNS<sub>2</sub>)(DMF) to give, eventually, decolorized solutions. Because the Mo(IV,VI) complexes were destroyed, product identification was not attempted. Similar reactivity of NO<sub>2</sub><sup>-</sup> with oxo Mo(IV,V) complexes has been reported.<sup>20-24</sup> A polymer-anchored oxo Mo(IV) complex is described as being oxidized to dioxo Mo(VI) with NO<sub>2</sub><sup>-</sup> formation,<sup>23</sup> supporting details of this encouraging transformation were not given. At present there are no well-defined synthetic systems that reproduce the stoichiometric nitrate reductase activity of reaction 4.

**Thermodynamic Aspects.** The preceding reactivity properties of Mo(IV, VI) complexes toward different substrates can be rationalized in terms of thermodynamic data.<sup>55,56</sup> When placed on a common scale by conversion to enthalpies for the reaction Red + 1/2 O<sub>2</sub>(g) → Ox, the series 25 is obtained. Because S-O

Red	Ox	ΔH, kcal/mol
NO <sub>2</sub> <sup>-</sup> (aq)	NO <sub>3</sub> <sup>-</sup> (aq)	25 <sup>55</sup>
Me <sub>2</sub> S(g)	Me <sub>2</sub> SO(g)	27 <sup>55</sup>
MoO(S <sub>2</sub> CNEt <sub>2</sub> ) <sub>2</sub> (soln)	MoO <sub>2</sub> (S <sub>2</sub> CNEt <sub>2</sub> ) <sub>2</sub> (soln)	35 <sup>56</sup>
MoO(LNS <sub>2</sub> )(DMF)(soln)	MoO <sub>2</sub> (LNS <sub>2</sub> )(soln)	
Me <sub>2</sub> SO(g)	Me <sub>2</sub> SO <sub>2</sub> (g)	52 <sup>55</sup>
Ph <sub>3</sub> P(soln)	Ph <sub>3</sub> PO(soln)	67 <sup>56</sup>

(25)

bond strengths in sulfoxides and sulfones are essentially independent of substituents,<sup>57</sup> ΔH data for the methyl derivatives should be widely applicable. The data are in agreement with, inter alia, the spontaneous oxidation of Ph<sub>3</sub>P by MoO<sub>2</sub>(S<sub>2</sub>CNEt<sub>2</sub>)<sub>2</sub><sup>26,42</sup> and reduction of Me<sub>2</sub>SO by MoO(S<sub>2</sub>CNEt<sub>2</sub>)<sub>2</sub>.<sup>26</sup> Given the occurrence of reaction 18 and the lack of reaction of MoO(LNS<sub>2</sub>)(DMF) with Me<sub>2</sub>SO<sub>2</sub>, the Red/Ox pair MoO(LNS<sub>2</sub>)(DMF)/MoO<sub>2</sub>(LNS<sub>2</sub>) can be placed between -35 and -52 kcal/mol on the ΔH scale, assuming entropy term differences are small. This position accounts for the occurrence of reactions 6 and 12 and indicates that NO<sub>3</sub><sup>-</sup> → NO<sub>2</sub><sup>-</sup> reduction by MoO(LNS<sub>2</sub>)(DMF) is thermodynamically feasible. This reaction may occur with the latter complex and MoO(S<sub>2</sub>CNEt<sub>2</sub>)<sub>2</sub>,<sup>58</sup> but follow-up reactions apparently prevent detection of NO<sub>2</sub><sup>-</sup> as a primary product. The ΔH data cannot be applied quantitatively owing to differences in physical phases of the Red/Ox pairs. Nonetheless, the order of pairs in series 25 is in agreement with known reactivity properties. Watt et al.<sup>56</sup> have provided an incisive analysis, based on thermochemical results, of the reactions of Mo(IV,VI) di-

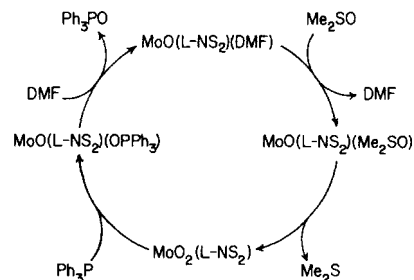


**Figure 7.** Catalytic cycle for the reduction of Me<sub>2</sub>SO using MoO(LNS<sub>2</sub>)(DMF) as the active catalyst and Ph<sub>3</sub>P as the reductant of its oxidized form, MoO<sub>2</sub>(LNS<sub>2</sub>).

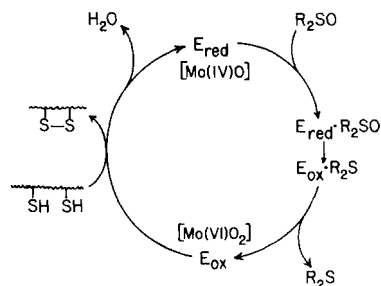


**Figure 8.** Proposed catalytic cycle for the enzymatic reduction of sulfoxides to sulfides.

thiocarbamates with biological substrates.

**Catalysis.** It has proven possible to couple reactions 6 and 12, with the result that the sulfoxide reduction reaction 20 can be made catalytic with use of Ph<sub>3</sub>P to regenerate the reactive Mo(IV) complex. With Me<sub>2</sub>SO as a model substrate, this process has been examined in detail. Both the reduction product, Me<sub>2</sub>S, and the associated oxidation product, Ph<sub>3</sub>PO, have been identified and quantitated. The catalytic cycle is shown in Figure 7. All aspects of the cycle have been demonstrated; formation of MoO(LNS<sub>2</sub>)(OPPh<sub>3</sub>) was shown by <sup>31</sup>P NMR results given earlier.<sup>9</sup>

The kinetics of the catalytic process have been followed by <sup>31</sup>P NMR spectroscopy. These studies demonstrate two important properties of the catalytic system. First, the turnover rate is linearly dependent on the MoO<sub>2</sub>(LNS<sub>2</sub>) concentration, indicating that catalysis is based on Mo-mediated oxo-transfer chemistry rather than some nonspecific process. Suitable controls demonstrated no reaction between sulfoxides and Ph<sub>3</sub>P in the absence of catalyst. Second, the initial rate is given by  $k[\text{MoO}_2(\text{LNS}_2)]$  with  $k = 6 \times 10^{-3} \text{ M}^{-1} \text{ s}^{-1}$ . This result shows that the catalytic rate is limited by the rate of oxo abstraction from MoO<sub>2</sub>(LNS<sub>2</sub>) by phosphine, as expected from the ratio 0.5:0.007 = 70:1 of the second-order rate constants for sulfoxide reduction and phosphine oxidation.

Although the system in Figure 7 is fairly robust, some catalyst decomposition is indicated by a gradual decrease in turnover rate and a decline in absorption intensity with time. The source of degradation appears to be reaction of MoO(LNS<sub>2</sub>)(DMF) with the (excess) Ph<sub>3</sub>P, as noted in separate kinetics studies of reaction 6. In the majority event the Mo(IV) complex is reoxidized to MoO<sub>2</sub>(LNS<sub>2</sub>) with concomitant sulfoxide reduction, but occasionally this species is decomposed, leading to reduced activity of the system. Nonetheless, in systems such as those in Figures 5 and 6, over 500 turnovers per equivalent of Mo catalyst have been observed. Somewhat related systems, for the aerial oxidation of tertiary phosphines and phosphites in the presence of dioxo Mo(VI) catalysts, have been devised.<sup>16,27b,59,60</sup> In such systems the inactive Mo(IV) species is converted to the active catalyst by reaction with dioxygen. Unlike the present system,  $\mu$ -oxo dimers are generated, and catalysis depends on the reversibility of a dimerization reaction such as 19.

(54) DeTitta, G. T.; Parthasarathy, R.; Blessing, R. H.; Stallings, W. *Proc. Natl. Acad. Sci. U.S.A.* **1980**, *77*, 333.

(55) Wagman, D. D.; Evans, W. H.; Parker, V. B.; Halow, I.; Bailey, S. M.; Schumm, R. H. "Selected Values of Chemical Thermodynamic Properties"; National Bureau of Standards: Washington, DC, 1968, *Technical Note* 270-3.

(56) Watt, G. D.; McDonald, J. W.; Newton, W. E. *J. Less-Common Met.* **1977**, *54*, 415. Data for the molybdenum dithiocarbamate complexes refer to 1,2-C<sub>2</sub>H<sub>4</sub>Cl<sub>2</sub> solutions.

(57) Mackle, H.; O'Hare, P. A. G. *Trans. Faraday Soc.* **1961**, *57*, 2119.

(58) Durant, R.; Garner, C. D.; Hyde, M. R.; Mabbs, F. E.; Parsons, J. R.; Richens, D. *J. Less-Common Met.* **1977**, *54*, 459. Results presented here dispute an earlier claim<sup>41</sup> that NO<sub>2</sub><sup>-</sup> is an observable reaction product.

(59) Barral, R.; Bocard, C.; S  r  e de Roch, I.; Sajus, L. *Tetrahedron Lett.* **1972**, 1693; *Kinet. Catal.* **1973**, *14*, 130.

(60) Speier, G. *Inorg. Chim. Acta* **1979**, *33*, 139.



**Summary and Prognosis.** Development of the catalytic cycle in Figure 7 for the Mo-mediated reduction of sulfoxides represents substantial progress in simulating, in a well-defined system, the oxo-transferase activity of reaction 5. For this system, several limitations and reservations are noted. A proposed cycle for enzymatic sulfoxide reduction is presented in Figure 8. Here allowance is made for the likely existence of enzyme complexes of the oxidized and reduced substrate. The most important difference compared to the scheme in Figure 7, however, is the source of electrons for reduction of the enzyme to its active form. A phosphine is obviously a nonphysiological reductant. Current evidence, summarized elsewhere,<sup>10</sup> suggests that the reducing power derives from the indicated  $2\text{RSH} = \text{RSSR} + 2\text{H}^+ + 2\text{e}^-$  couple of cysteinyl-containing proteins. Consequently, a more physiologically realistic cycle would incorporate this couple. Only *d*-biotin *d*-(S-oxide) reductase, among the biological sulfoxide reducing activities summarized above, has been shown to be a Mo-dependent enzyme. Its purification and structural interrogation of its Mo site will be required before any conclusions can be drawn concerning similarities with  $\text{MoO}(\text{LNS}_2)(\text{DMF})$  and  $\text{MoO}_2(\text{LNS}_2)$ . What can be said at this stage of evolution of the oxo-transferase modeling problem is that these complexes are reasonable structural approaches to the catalytic sites of other enzymes of this general type. Further challenges include the development of similarly structurally credible systems capable of the oxo-transfer activities of reactions 1-4.

In the synthetic analogue approach to the active sites of metallobiomolecules, a desirable first step is the attainment of an

acceptable structural model.<sup>61</sup> It is encouraging to witness recently the development of reactivity models for enzyme such as carboxypeptidase A,<sup>62,63</sup> carbonic anhydrase,<sup>64</sup> urease,<sup>65</sup> cytochrome P-450,<sup>66</sup> tyrosinase,<sup>67</sup> and superoxide dismutase.<sup>68</sup> Evolvement of the sulfoxide reducing system described here, which features substrate saturation kinetics, transformation of the physiological substrate 1, and a well-defined catalyst capable of turnover of hundreds of equivalents of a model substrate without intervention of a physiologically unrealistic  $\mu$ -oxo Mo(V) dimer, provides an additional contribution to this endeavor.

**Acknowledgment.** This research was supported by NSF Grant CHE 81-06017. We thank Don Wink for assistance with the stoichiometric <sup>31</sup>P NMR studies.<sup>9</sup>

(61) Ibers, J. A.; Holm, R. H. *Science (Washington, D.C.)* **1980**, *209*, 223.

(62) Breslow, R.; Chin, J.; Hilvert, D.; Trainor, G. *Proc. Natl. Acad. Sci. U.S.A.* **1983**, *80*, 4585.

(63) Groves, J. T.; Chambers, R. R., Jr. *J. Am. Chem. Soc.* **1984**, *106*, 630.

(64) Brown, R. S.; Curtis, N. J.; Huguet, J. *J. Am. Chem. Soc.* **1981**, *103*, 6953. Brown, R. S.; Salmon, D.; Curtis, N. J.; Kusuma, S. *Ibid.* **1982**, *104*, 3188. Slebocka-Tilk, H.; Cocho, J. L.; Frakman, Z.; Brown, R. S. *Ibid.* **1984**, *106*, 2421.

(65) Blakeley, R. L.; Treston, A.; Andrews, R. K.; Zerner, B. *J. Am. Chem. Soc.* **1982**, *104*, 612.

(66) Groves, J. T.; Nemo, T. E. *J. Am. Chem. Soc.* **1983**, *105*, 5786, 6243.

(67) Karlin, K. D.; Cruse, R. W.; Gultneh, Y.; Hayes, J. C.; Zubieta, J. *J. Am. Chem. Soc.* **1984**, *106*, 3372 and references therein.

(68) Strothkamp, K. G.; Lippard, S. J. *Acc. Chem. Res.* **1982**, *15*, 318 and references therein.

## Synthesis, Structural Characterization, and Stereospecificity in the Formation of Bimetallic Rhodacarborane Clusters Containing Rh-H-B Bridge Interactions

Paul E. Behnken, Todd B. Marder, R. Thomas Baker, Carolyn B. Knobler, Michael R. Thompson, and M. Frederick Hawthorne\*

Contribution from the Department of Chemistry and Biochemistry, University of California, Los Angeles, Los Angeles, California 90024. Received July 11, 1984

**Abstract:** Reactions of  $[\text{Rh}(\text{COD})(\text{PR}_3)\text{Cl}]$  ( $\text{COD} = \eta^4\text{-1,5-cyclooctadiene}$ ;  $\text{R} = \text{Ph}$ ;  $\text{Et}$ ;  $\text{Ph}$ ,  $\text{Me}$ ) with  $[\text{nido-7-R-7,8-C}_2\text{B}_9\text{H}_{11}]^-$  [ $\text{R} = \text{H}$ ,  $\text{Ph}$ ,  $7'\text{-nido-7',8'-C}_2\text{B}_9\text{H}_{11}$ ] resulted in the formation of bimetallic rhodacarborane clusters containing Rh-Rh bonds supported by Rh-H-B interactions.  $[\text{Rh}(\text{PPh}_3)_2\text{C}_2\text{B}_9\text{H}_{11}]_2$  (**2**) is formed stereospecifically as the nature of the Rh-H-B interactions determines a specific stereoisomer and of the six possible only the structure of **2** is observed. The synthesis, characterization, and X-ray structure determinations of analogues of **2** containing differing phosphine ligands demonstrate this stereospecificity to be of thermodynamic origin, arising from polyhedral repulsions on adjacent carborane ligands. The characterization of  $[\text{Rh}(\text{PET}_3)_2(\text{H})\text{C}_2\text{B}_9\text{H}_{10}\text{-Rh}(\text{CODH})\text{C}_2\text{B}_9\text{H}_{10}]$  (**8**) as well as experiments observing the formation of **2** result in a general mechanism for their formation involving hydrogenation of the COD ligand to cyclooctene via phosphine ligand disproportionation.  $[\text{Rh}(\text{PPh}_3)_2\text{C}_2\text{B}_9\text{H}_{11}]_2$  (**2**) crystallizes in the triclinic space group  $P\bar{1}$  with unit cell parameters  $a = 11.118$  (2) Å,  $b = 13.456$  (3) Å,  $c = 18.390$  (3) Å,  $\alpha = 93.09$  (2)°,  $\beta = 76.22$  (1)°,  $\gamma = 76.90$  (2)°,  $Z = 2$ .  $[\text{Rh}(\text{PET}_3)_2\text{C}_2\text{B}_9\text{H}_{10}]_2$  (**3**) crystallizes in the monoclinic space group  $P2_1/c$  with unit cell parameters  $a = 11.153$  (6) Å,  $b = 15.228$  (9) Å,  $c = 18.844$  (10) Å,  $\beta = 91.83$  (2)°,  $Z = 4$ .  $[\text{Rh}(\text{PPh}_3)_2\text{C}_2\text{B}_9\text{H}_{10}\text{C}_6\text{H}_5]_2$  (**5**) crystallizes in the monoclinic space group  $P2_1/c$  with unit cell parameters  $a = 18.035$  (6) Å,  $b = 13.156$  (4) Å,  $c = 26.905$  (8) Å,  $\beta = 113.34$  (2)°,  $Z = 4$ .  $[\text{Rh}(\text{PET}_3)_2(\text{H})\text{C}_2\text{B}_9\text{H}_{10}\text{-Rh}(\text{CODH})\text{C}_2\text{B}_9\text{H}_{10}]$  (**8**) crystallizes in the monoclinic space group  $P2_1/n$  with unit cell parameters  $a = 14.043$  (7) Å,  $b = 32.638$  (13) Å,  $c = 10.059$  (4) Å,  $\beta = 98.98$  (3)°,  $Z = 4$ .

In the course of our mechanistic study<sup>1</sup> of the homogeneous hydrogenation and isomerization of olefins catalyzed by *closo*-

3,3-( $\text{PPh}_3$ )-3-(H)-3,1,2-RhC<sub>2</sub>B<sub>9</sub>H<sub>11</sub>] (**1**) we reported the structure of a dimeric rhodacarborane,  $[\text{Rh}(\text{PPh}_3)_2\text{C}_2\text{B}_9\text{H}_{11}]_2$  (**2**), initially